Transmutation of Transuranic Elements as Solid Coating in Molten Salt Reactor Fuel Channel

R Andika Putra Dwijayanto[1*]**, Fitria Miftasani**[1]**, Andang Widi Harto**[2]

[1] *Research Centre for Nuclear Reactor Technology, Research Organisation for Nuclear Energy, National Research and Innovation Agency, Building No. 80 BJ Habibie Science and Technology Area, South Tangerang 15314, Indonesia*
[2] *Department of Nuclear Engineering and Physics Engineering, Faculty of Engineering, Universitas Gadjah Mada, Jl. Grafika No. 2, Yogyakarta 55281, Indonesia*

ARTICLE INFO

A B S T R A C T

The accumulation of spent nuclear fuel (SNF) is presently considered a hindrance to the massive deployment of nuclear power plants, especially regarding the transuranic (TRU) elements. Eliminating TRU through transmutation is one of the most feasible alternatives as a technical solution to solve the issue. This study explores the possibility of TRU transmutation using a molten salt reactor (MSR) in a heterogeneous configuration, where a solid TRU is coated inside the fuel channel filled with liquid salt fuel. Such a configuration is proposed to allow higher TRU loading into the fluoride salt mixture without compromising the safety of the reactor. TRU coating was applied in consecutively outward radial fuel channel layers with coating thicknesses of 2.5 mm and 5 mm. The calculation was performed using MCNP6.2 radiation transport code and ENDF/B-VII.0 neutron cross-section library. From the results, TRU coating with a smaller thickness and positioned closer to the centre of the core exhibit higher transmutation efficiency due to exposure to the higher neutron flux. The highest transmutation efficiency was achieved at 67.93% after 160 days of burnup. This shows a potential of achieving highly efficient TRU using heterogeneous configuration in MSR core.

1. INTRODUCTION*

Spent nuclear fuel (SNF) is often considered one of the hindrances to the global expansion of nuclear power. The primary issue in the SNF lies in the transuranic (TRU) elements, which consist of plutonium (Pu) and minor actinide (MA) isotopes [1]. Many TRU isotopes have a long half-life so that the time required for them to decay until the remaining radioactivity equals the reference value spans up to 130,000 years [2]. Most of the radioactivity would be in the form of alpha and beta radiation, which pose a risk only if ingested or inhaled. Potential human intake of those radionuclides through several layers of radioactive waste barrier in the final disposal is tremendously small, indicating a small long-term risk of SNF disposal [3]. Nonetheless, the present narration on SNF especially TRU is that the long-term disposal is marred with uncertainty and that it would be safer to reduce or even eliminate the TRU altogether [4–7] to prevent a distant future, high-uncertainty, and highly improbable problem, if any, from happening.

Assuming that the above reasoning is sound, there are various alternatives to minimize the TRU generated from nuclear power generation.

---

*Corresponding author. Tel./Fax.: (021) 7560912
E-mail: rand002@brin.go.id

Considering the front-end of nuclear power generation, the option is to replace uranium as a primary fuel to thorium [8–11]. Since thorium has smaller atomic and mass numbers than uranium, the former must capture at least seven successive neutron captures prior to transmuting into TRU. This significantly reduces the TRU generation. However, thorium fuel cycle is immature and cannot sustain without external fissile nuclide, as thorium has no fissile isotope. U-233, which is generated from thorium capture of neutron, is non-existent in nature due to its shorter half-life than U-235 [12]. Introducing thorium in uranium fuel cycle can reduce the resulting TRU generation, at the expense of higher uranium enrichment [13–15]. Notwithstanding, abandoning uranium for thorium only to reduce TRU waste is a waste of resource.

From back-end consideration, TRU can be eliminated through transmutation in nuclear reactor or accelerator-driven system (ADS) [16]. In term of resource utilisation, back-end TRU transmutation allows the exploitation of uranium potential instead of discarding it for the sake of waste minimisation. In nuclear reactor, transmutation can be performed in both research reactor [17, 18] and power reactor with various types of fission reactors. Conventional light water reactors (LWRs) have been studied to transmute TRU, either by using TRU wholly as a fuel rod [6, 19–21] or as coating layer [7, 22]. Combining TRU with thorium ensures negative yield of TRU [23], due to the reason mentioned previously.

TRU elimination was also analysed in Generation IV reactors, such as lead-cooled fast reactor [5], sodium-cooled fast reactor [24], high temperature gas-cooled reactor [25], and molten salt reactor [26, 27]. Fast-spectrum reactors possess an advantage in term of high neutron energy which allows the fission of various TRU elements. As fission reaction results in short-lived fission products, transmutation through fission can assure the resulting radionuclides to be rapidly decays into stable nuclide. However, thermal-spectrum reactors also have advantage as neutron capture probability is larger in thermal energy region, although neutron capture reaction (n, γ) does not always result in short-lived radionuclides [2].

Molten salt reactor (MSR) is a Generation IV nuclear reactor design with distinctive characteristics in form of liquid salt compound as fuel. The use of liquid fuel gives MSR unique characteristics, such as high temperature operation with low system pressure, the elimination of core melting and pressure-initiated accidents, and online fuel reprocessing. Due to the use of liquid fuel as well, MSR can be designed either as thermal-spectrum or fast-spectrum reactor, though the early development of MSR and most of current MSR developments are thermal-spectrum [28, 29].

MSR capability as TRU transmuter has been analysed both in thermal and fast neutron spectra. In thermal spectrum, TRU transmutation was modelled by mixing the TRU in the fuel salt. This method is limited by the solubility of trifluoride compound of the TRU elements in fluoride-based salt used in thermal MSR [30] and the positive temperature feedback induced by Pu isotopes [31]. An alternative to this method is by using heterogeneous method, where the TRUs are separated from the fuel salt as a solid elements. Such heterogeneous configuration was studied in fast chloride MSR [2], but none has been studied in thermal fluoride. This research was performed as an initial assessment of the potential of TRU transmutation as a heterogeneous configuration in thermal MSR. A one fluid MSR model was used as the model of this study.

2. REACTOR DESCRIPTION

To analyse the feasibility of TRU transmutation as a coated layer, a generic single fluid MSR model (see Fig. 1) was used. The core has a single fluid stream with single fuel channel size. The fuel enters the core from the top plenum, fissioned in the reactor core, and flows down into the bottom plenum to the primary loop. The MSR model is a large power MSR with thermal power of 2,250 MWt, the same with Molten Salt Breeder Reactor (MSBR) [32] and Single fluid Double Zone-Thorium Molten Salt Reactor (SD-TMSR) [33]. Its nominal operational temperature is 900K. The MSR core is moderated by graphite with density of 1.86 g/cm^3, similar to that of MSBR [34]. The active core is surrounded by axial and radial graphite reflectors with the same density. Radial boron carbide layer is placed outside the radial reflector to protect the vessel from neutron bombardment.
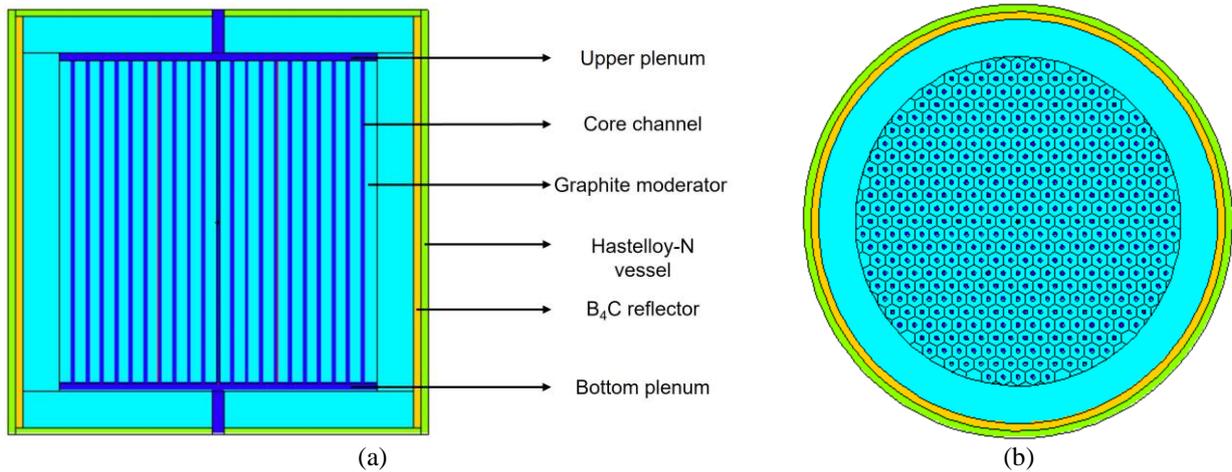
Fig. 1. Generic molten salt reactor model (a) axial, (b) radial

The fuel salt composition (in %mole) is 71LiF-16BeF$_2$-13(U,Th)F$_4$. The Li-7 isotope in LiF is enriched to 100% to prevent parasitic capture by Li-6. U-233 is used as the fissile driver, accompanied by Th-232 as the fertile nuclide. The core channel is distributed throughout the core with single dimension,

a radius of 3 cm. This singular fuel channel size is more suitable for non-breeder MSR due to limited neutron economy.

Core parameters of the MSR is summarised in Table 1.

Table 1. Core parameters of molten salt reactor

Parameter	Value
Thermal power (MWt)	2,250
Fuel composition (%mole)	71LiF-16BeF$_2$-13(U,Th)F$_4$
Fuel temperature (K)	900
Fuel density (g/cm^3)	3.14
Graphite density (g/cm^3)	1.86
B$_4$C density (g/cm^3)	2.52
B$_4$C thickness (cm)	10
Core vessel thickness (cm)	10
Core height and diameter (cm)	440
Hexagonal side length of graphite moderator (cm)	10
Core channel radius (cm)	3
Radial reflector thickness (cm)	50
Axial reflector thickness (cm)	50

The TRU is introduced into the reactor core in a solid form, creating a heterogeneous configuration between the fuel salt and TRU elements. In this model, the TRU is coated onto the inner surface of fuel channel as (TRU)O$_2$ (see Fig. 2), replacing part of the fuel instead of graphite. This was done to kept fuel volume the same. The TRU coating is in direct contact with the fuel salt and thereby subject to corrossion and fuel intrusion. The effect of chemical interaction between fuel salt and (TRU)O$_2$ is yet to be investigated in the literatures, and its effect on the reactor physics parameter is presently unknown. The TRU isotopic vector is provided in Table 2.
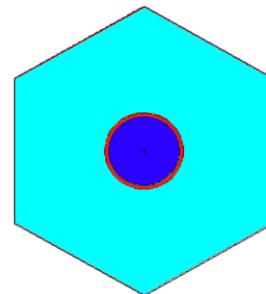
Fig. 2. Transuranic-coated molten salt reactor fuel channel. Cyan is graphite moderator, red is transuranic coating, blue is fuel salt.

Table 2. Transuranic isotopic vectors (%wt) [35]

Isotope	Weight Fraction
Pu-238	1.42
Pu-239	51.98
Pu-240	23.91
Pu-241	7.88
Pu-242	4.80
Np-237	4.23
Am-241	4.76
Am-243	0.85
Cm-242	0.032
Cm-243	0.001
Cm-244	0.126
Cm-245	0.007
Cm-246	0.001

3. CALCULATION METHOD

The neutronic calculations was performed using MCNP6.2 multipurpose radiation transport code and ENDF/B-VII.0 continuous neutron cross section library. MCNP is capable of modelling a complex geometry without simplification, allowing more accurate prediction of the reactor physics characteristics. Previously, MCNP was used to calculate neutronic parameters of MSBR [36, 37], Integral Molten Salt Reactor (IMSR) [38], MSR-FUJI [39], TMSR-500 [40, 41], and PCMSR [42]. Therefore, MCNP can be considered to be suitable to calculate the neutronic parameters of an MSR, despite the calculation was performed in a quasi-static condition.

One distinctive feature of MSR is the capability of online fuel reprocessing. This allows the MSR to remove unwanted fission products and actinides from the reactor core to maintain the neutron economy. This also reduces the excess reactivity requirement to maintain criticality. However, MCNP6.2 lacks the defining feature to properly simulate the online reprocessing. Thus, a simple burnup calculation using CINDER90 module was imposed instead, so that sufficiently large excess reactivity is added at the beginning of cycle (BOC) to compensate for the loss of reactivity throughout the burnup. This is especially important as the generic single fluid MSR model used here has poor breeding performance compared to single fluid-dual zone MSR configuration [43].

A total of 2 million neutron histories was used, so that the standard deviation of the effective multiplication factor is around ± 44-47 pcm. U-233 molar fraction was set to 1%mole and Th-232 to 12%mole. The cutoff of burnup calculation is one step prior to subcriticality, as a reasonable limit of reactor operation. Each burnup step was calculated at 20 days interval to prevent inaccuracies in neutron flux calculation.

(a)	(b)
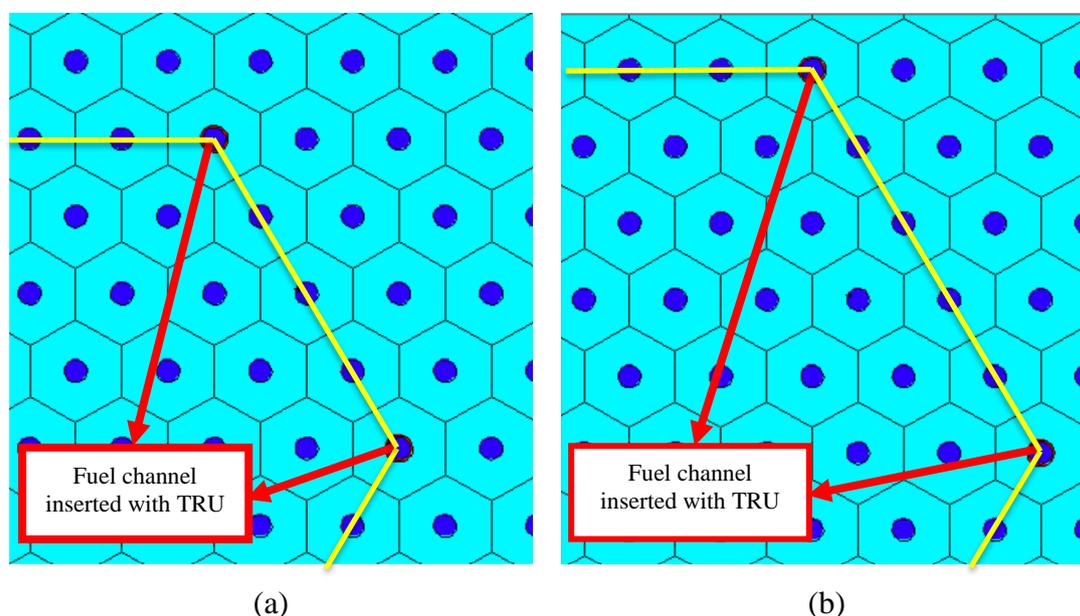
Fig. 3. Placement of TRU-coated fuel channel, yellow lines show the ring position (a) Ring 6, (b) Ring 7

The placement of TRU coating is illustrated in Fig. 3. Here, we denote the radial graphite fuel channel layer as "Ring," where lower number rings are closer to the centre of the reactor and higher number rings are placed on the outermore of the lower number. For this initial assessment, the coated fuel channels are placed in Ring 3 until Ring 7, to provide the TRUs with sufficient neutron flux. Ring 2 was not used as it has no fuel channels in-between the TRU channels, so that the TRU channels are too closely packed.

At each Ring, six fuel channels located on each hexagonal point of the Ring are coated with TRU. Two coating thicknesses were used, 2.5 mm and 5 mm, resulting in a total TRU load of 20.16 kg and 38.57 kg, respectively. The thicknesses were chosen as a reasonable TRU coating thickness, so that not particularly thick that results in self-shielding effect but also not too thin so that TRU loading was compromised. Fission products and TRU can also migrate into the fuel salt in this manner. However, there is a lack of literature discussing the migration of fission product from the solid oxide fuel to the liquid fluoride salt as it has never been done before.

Transmutation efficiency (TE) is calculated using Eq. 1.

$$TE = \frac{TRU_{BOC} - TRU_{EOC}}{TRU_{BOC}} \qquad (1)$$

where TRU_{BOC} is the mass of TRU at the BOC and TRU_{EOC} is the mass of TRU at the end of cycle (EOC).

4. RESULTS AND DISCUSSION

Figure 4 shows the profile of the effective multiplication factor (k_{eff}) with different coating thicknesses and ring placements. The figure shows that the k_{eff} value with a coating thickness of 2.5 mm is higher compared to 5 mm. This value difference is associated with higher neutron absorption in the 5 mm coating thickness due to larger MA loading, resulting in a lower k_{eff} value. The highest k_{eff} value for the 2.5 mm coating thickness is found in Ring 5. Meanwhile, the k_{eff} value for the 5 mm coating thickness is the lowest in Ring 7, but the decrease is not linear.

Fluctuations in the k_{eff} values for the same coating thicknesses are related to statistical uncertainties in criticality calculation. Thus, given the uncertainties and looking at the trend, insertion of 2.5 mm of TRU coating did not significantly alter the k_{eff} values against ring placement, whilst insertion of 5 mm of TRU coating resulted in lowering of k_{eff} in the higher ring number. The latter is caused by lower neutron flux in rings farther from core centre, so less fission induced from the fissile Pu isotopes in the coating layers.
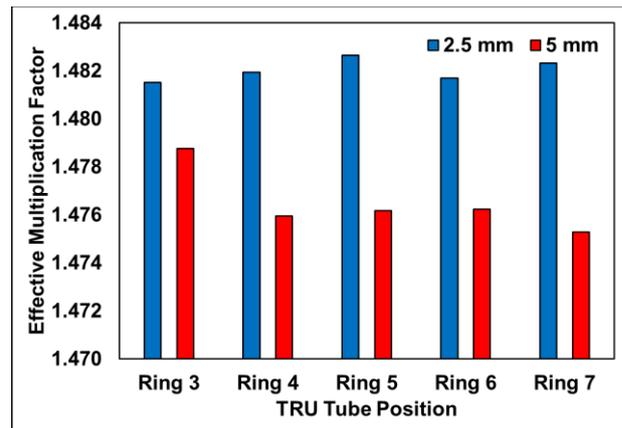
Fig. 4. Effective multiplication factor with different coating thicknesses and ring placement

On the other hand, Fig. 5 shows the profile of average lethargy energy causing fission (ALEF) with different coating thicknesses and ring placements. ALEF represents the measure of neutron energy change when interacting with matter. The profile of ALEF decreases from the innermost to the outermost ring for both thicknesses. The decrease in ALEF values is higher for the 5 mm thickness than for the 2.5 mm thickness. This value indicates that in rings 3-4, the ALEF value for the 5 mm thickness is higher than the 2.5 mm thickness, whilst in rings 5-7, the ALEF value for the 5 mm thickness is lower than the 2.5 mm thickness.

The difference in average lethargy energy values between these two thicknesses is due to the difference in neutron absorption probabilities. The profile shows a faster decrease in average lethargy energy for the 5 mm thickness, indicating a more significant change in neutron energy than the 2.5 mm coating thickness. This implies that neutrons are more efficiently thermalised in the thicker coating as the placement is getting farther from core centre.
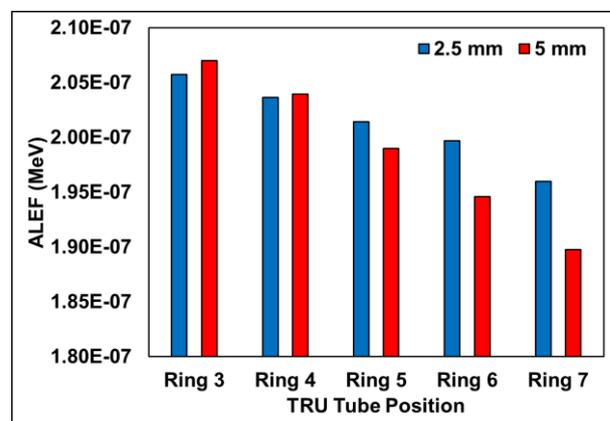
Fig. 5. Average lethargy energy causing fission with different coating thicknesses and ring placement

The evolution of the k_{eff} values for both thicknesses is shown in Figs. 6a and 6b. Both figures exhibit a decreasing profile with cutoff operating time at 160 days. The decrease in k_{eff} values over burnup time can be attributed to several factors, including the reduction in fuel fraction and the accumulation of neutron-absorbing fission products, whilst the new fissile bred from Th is unable to compensate. Applying gaseous fission product removal to expunge Xe and Kr isotopes will extend the burnup time, but nonetheless insufficient to continuously maintain criticality.

The difference in k_{eff} values for each ring is relatively insignificant, and even less so in 5 mm thickness. The same observation was made for the k_{eff} values between the two thicknesses, whose profiles do not significantly differ. Therefore, in term of actual burnup calculations, TRU insertion for both thicknesses do not particularly affect the length of critical state.

The profile of U-233 burnup evolution with different coating thicknesses is depicted in Fig. 7. MSR core with both thicknesses exhibit a similar U-233 burnup profile, increasing with operating time, with insignificant differences in values. The variation in burnup values for each ring placement is also observed to be insignificant. U-233 burnup level, thus, is shown to be unaffected by TRU insertion. This shows that TRU insertion offered little to total core power and total core burnup. This is understandable as TRU loading is comparably smaller than U-233.
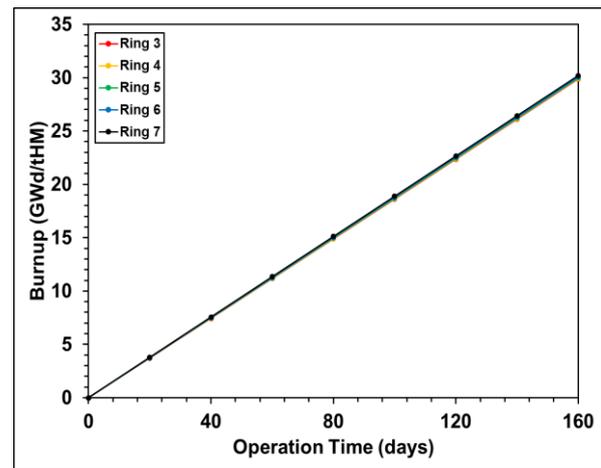
(a)
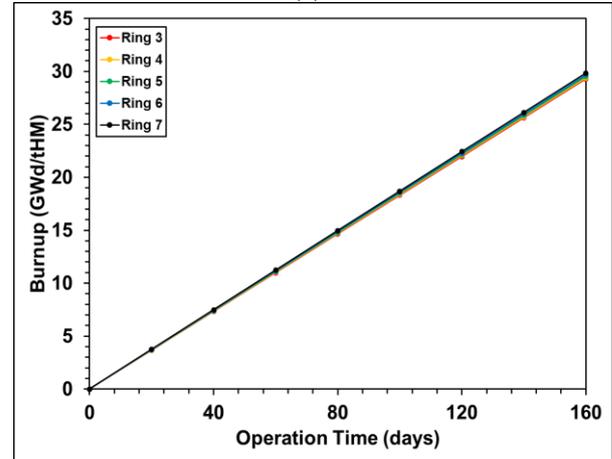
(b)

Fig. 7. U-233 burnup evolution with different coating thicknesses (a) 2.5 mm, (b) 5 mm.

The difference in TRU burnup profiles with different coating thicknesses is shown in Fig. 8. The TRU burnup profiles for both coating types show an increasing trend with operating time. Unlike U-233 burnup, TRU burnup profiles exhibit a notable difference. TRU burnup level for the 2.5 mm coating thickness is higher than the 5 mm coating thickness. This value implies that the 2.5 mm coating thickness exhibits better transmutation, due to smaller thickness and thereby lower TRU load, allowing neutrons to transmute a larger fraction of TRU.

(a)

(b)

Fig. 6. Evolution of effective multiplication factor throughout burnup with different coating thicknesses (a) 2.5 mm, (b) 5 mm.

Additionally, the TRU burnup value is highest in Ring 3 for all thicknesses, and decreased in subsequent rings. This is due the TRU in Ring 3 is exposed to higher neutron flux due to its proximity to the core centre. The TRU burnup in day 160 far exceeds the design burnup of oxide fuels, which is below 100 GWd/tHM. This will undoubtedly create a structural problem such as cracking. Nonetheless, fission products released from such scenario will be safely bonded into stable fluoride salt in the core.

(a)

(b)
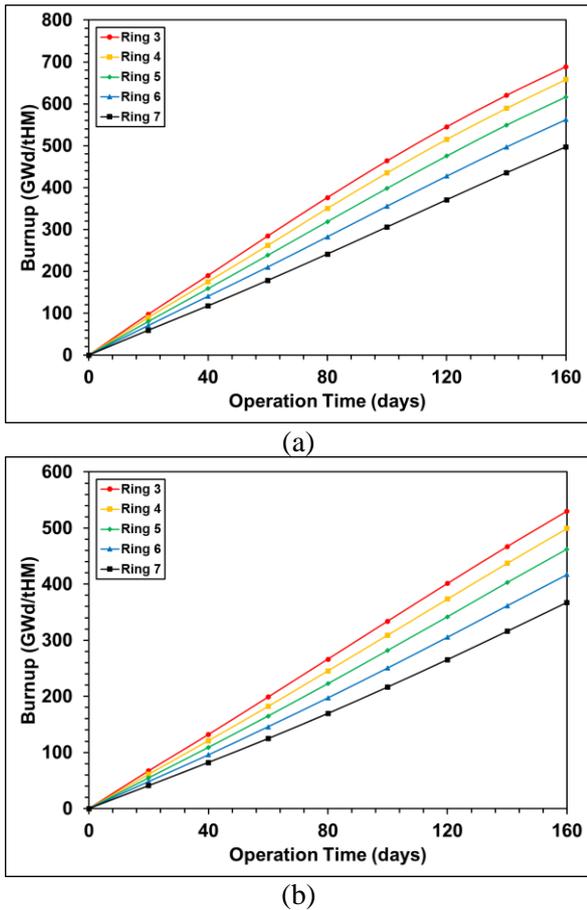
Fig. 8. TRU burnup evolution with different coating thicknesses (a) 2.5 mm, (b) 5 mm.

Figs. 9a and b illustrate the evolution of Pu isotopic proportions during the operation of nuclear fuel in the reactor over time for both coating thicknesses. Pu-239 is one of the essential isotopes in nuclear energy production. Pu-239 undergoes further fission reactions during burnup and contributes to energy generation, producing other Pu isotopes such as Pu-240, Pu-241, and Pu-242. In both coating thicknesses, it can be observed that the mass of Pu-239 significantly decreases with burnup time, as Pu-239 has large fission cross section. On the other hand, Pu-240 and Pu-242 tend to have less favorable neutronic characteristics, but an insignificant increase in both isotopes is observed due to neutron capture. The former is then decreased

as its transmutation rate surpassed its replenishment rate as its precursor, Pu-239, rapidly depleted.

(a)

(b)
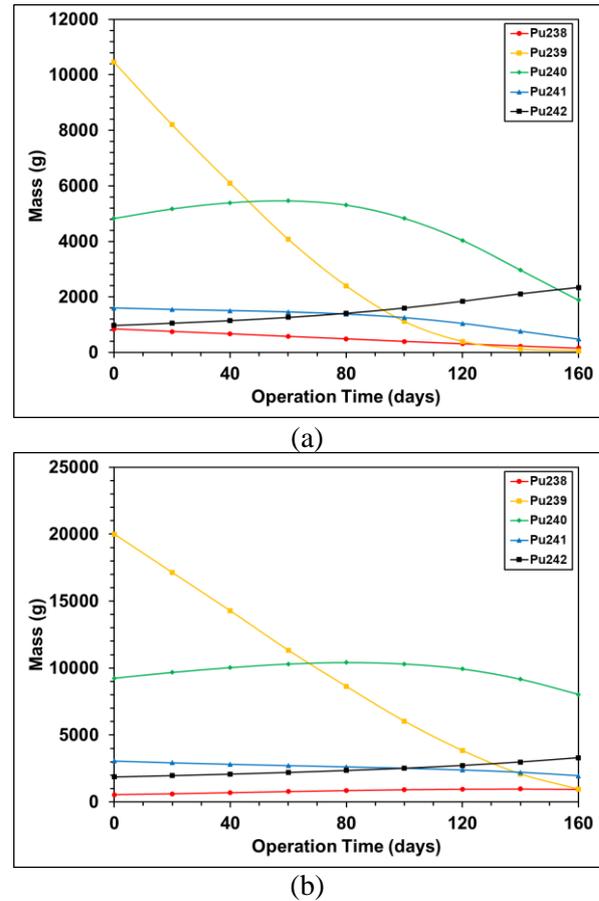
Fig. 9. Evolution of Pu isotopes throughout burnup with different coating thicknesses (a) 2.5 mm, (b) 5 mm.

As transmutation rate is lower in 5 mm TRU thickness, Pu-240 decrease is not particularly steep compared to 2.5 mm TRU thickness. Thus, Pu-240 remains the most dominant isotope in 5 mm TRU thickness, whilst Pu-242 is the most dominant Pu isotope in 2.5 mm thickness. Both are fertile isotopes, but Pu-242 has smaller capture cross section and once captured a neutron, it transmutes into unstable Pu-243. The significantly less probability of creating a new fissile isotope gives 2.5 mm TRU thickness an advantage.

Figure 10 shows the changes of MA isotopes concentration throughout burnup with different coating thicknesses. The profiles of MA mass for both coating thicknesses exhibit a similar trend, although the values vary. Generally, the presence of a more significant amount of MA can affect the reactivity characteristics of the reactor since MAs can act as significant neutron absorbers (see Fig. 4).
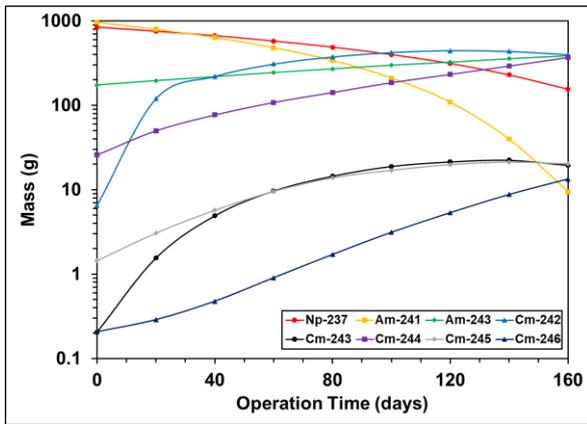
(a)
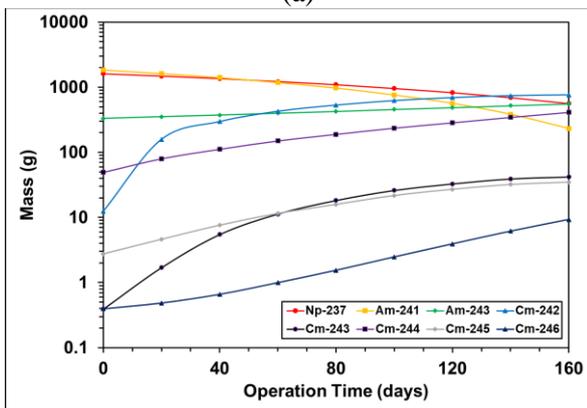
(b)

Fig. 10. Evolution of MA isotopes throughout burnup with different coating thicknesses (a) 2.5 mm, (b) 5 mm. Scale in logarithmic.

(a)

(b)

Fig. 11. TRU mass evolution with different coating thicknesses (a) 2.5 mm, (b) 5 mm.

Np-237 and Am-241 are considered as MA isotopes with high significance. Both are transmuted with a negative rate, meaning that their mass at EOC is lower than BOC. Am-241 was transmuted faster, and steeper in 2.5 mm TRU thickness, due to its larger capture cross section. Other MA isotopes, meanwhile, have their transmutation rate positive. This is due their transmutation rates are comparably slower than their replenishment rates, as their precursor isotopes are still high in concentration.

In total, TRU mass evolution with different coating thicknesses is depicted in Fig. 11. The influence of the coating thickness causes the TRU mass with a 5 mm thickness to be larger than the 2.5 mm thickness. Both thicknesses exhibit a decreasing trend, with the highest remaining TRU mass found in Ring 7 for both thicknesses. The latter is the result of lower neutron flux in the outermore rings, which reduces transmutation rate.

In spite of positive transmutation rate found in several Pu and MA isotopes, most of important TRU isotopes are almost completely annihilated, so that total TRU transmutation rate is negative. The transmutation rate ranges between 50.75-67.93% for 2.5 mm TRU thickness and between 38.29-53.92% for 5 mm TRU thickness. Longer MSR operation will definitely reduces the TRU even further. However, the effect of almost total burnup in structural aspect of oxide coating and its chemical interaction with molten salt as a whole, not just fission products, is presently unknown.

5. CONCLUSION

TRU transmutation using heterogeneous configuration in an MSR shows a potential to be applied in the future. Using two different TRU coating thicknesses, the TRU can be transmuted up to 67.93% from its initial loading. The results show that to achieve higher transmutation rate, the TRU thickness should be small, in this study 2.5 mm, and placed in the close proximity of the core centre in order to expose the TRU with higher neutron flux. Overall, this heterogeneous configuration is promising, but requires deeper analysis especially in

terms of TRU loading, coating materials, and TRU isotopic compositions. The impact of TRU insertion on the reactivity coefficients must also be investigated in future works.

ACKNOWLEDGEMENT

AUTHOR CONTRIBUTION

R. Andika Putra Dwijayanto conceptualise the research, develop the methodology, curate the data, performed the analysis, and write the manuscript. Fitria Miftasani performed the analysis and write the manuscript. Andang Widi Harto provide the software and supervise the research. All authors read and approve the final version of the paper.

REFERENCES

1. Dwijayanto R.A.P., Alfarisie M. Preliminary Study on Minor Actinide Incineration in RSG-GAS without Isotope Separation. GANENDRA Maj. IPTEK Nukl. 2021. **24**(2):85.
2. Li X., Cui D., Hu G., Cai X., Chen J. Potential of transuranics transmutation in a Thorium-based Chloride Salt Fast Reactor. Int. J. Energy Res. 2022. **46**(12):16461–75.
3. Cohen B.L. The Nuclear Energy Option: An Alternative for the 90s. New York:Springer New York; 1990.
4. You W.S., Hong S.G. A Neutronic Study on Advanced Sodium Cooled Fast Reactor Cores with Thorium Blankets for Effective Burning of Transuranic Nuclides. Nucl. Eng. Des. 2014. **278**:274–86.
5. Liu B., Han J., Liu F., Sheng J., Li Z. Minor Actinide Transmutation in the Lead-cooled Fast Reactor. Prog. Nucl. Energy. 2020. **119**:103148.
6. Liu B., Jia R., Han R., Lyu X., Han J., Li W. Minor Actinide Transmutation Characteristics in AP1000. Ann. Nucl. Energy. 2018. **115**:116–25.
7. Hu W., Jing J., Bi J., Zhao C., Liu B., Ouyang X. Minor Actinides Transmutation on Pressurized Water Reactor Burnable Poison Rods. Ann. Nucl. Energy. 2017. **110**:222–9.
8. Zuhair, Andika Putra Dwijayanto R., Suwoto, Setiadipura T. The Implication of Thorium Fraction on Neutronic Parameters of Pebble Bed Reactor. Kuwait J. Sci. 2021. **48**(3)
9. Wojciechowski A. The U-232 Production in Thorium Cycle. Prog. Nucl. Energy. 2018. **106**(March):204–14.
10. Arias F.J. Minimization of U-232 Content in Advanced High-conversion Multirecycling Thorium Reactors by Blanket Fragmentation. Prog. Nucl. Energy. 2013. **67**:18–22.
11. Ganda F., Arias F.J., Vujic J., Greenspan E. Self-Sustaining Thorium Boiling Water Reactors. Sustainability. 2012. **4**:2472–97.
12. Dwijayanto R.A.P., Hermawan D.P. Investigation on Inherent Safety of One Fluid-Molten Salt Reactor (OF-MSR) With Various Starting Fuel. J. Teknol. Reakt. Nukl. Tri Dasa Mega. 2020. **22**(2):54.
13. Uguru E.H., Sani S.F.A., Khandaker M.U., Rabir M.H. Investigation on the Effect of 238U Replacement with 232Th in Small Modular Reactor (SMR) Fuel Matrix. Prog. Nucl. Energy. 2020. **118**(July 2019):103108.
14. Zhu G., Zou Y., Yan R., Tan M., Zou C., Kang X., et al. Low Enriched Uranium and Thorium Fuel Utilization under Once-through and Offline Reprocessing Scenarios in Small Modular Molten Salt Reactor. Int. J. Energy Res. 2019. **43**(11):5775–87.
15. Korkmaz M.E., Agar O., Büyüker E. Burnup Analysis of the VVER-1000 Reactor using Thorium-based Fuel. Kerntechnik. 2014. **79**(6):478–83.
16. Zhou S., Wu H., Zheng Y. Flexibility of ADS for Minor Actinides Transmutation in Different Two-stage PWR-ADS Fuel Cycle Scenarios. Ann. Nucl. Energy. 2018. **111**:271–9.
17. Setiawan M.B., Kuntjoro S. Preliminary Analysis of High-Flux RSG-GAS to Transmute Am-241 of PWR's Spent Fuel in Asian Region. in: *Journal of Physics: Conference Series*. 2018. p. 12004.
18. Setiawan M.B., Kuntjoro S., Husnayani I., Udiyani P.M., Surbakti T. Evaluation on Transmutation of Minor Actinides Discharged from PWR Spent Fuel in the RSG-GAS Research Reactor. Malaysian J. Fundam. Appl. Sci. 2019. **15**(4):577–9.
19. Hu W., Liu B., Ouyang X., Tu J., Liu F., Huang L., et al. Minor Actinide Transmutation on PWR Burnable Poison Rods. Ann. Nucl. Energy. 2015. **77**:74–82.
20. Hussain M., Sohail M. Feasibility Study of Transmutation of Minor Actinides in PWR Fuel Assembly. in: *ICET 2016 - 2016 International Conference on Emerging Technologies*. 2017. pp. 16–9.
21. Washington J., King J. Optimization of Plutonium and Minor Actinide Transmutation in an AP1000 Fuel Assembly via a Genetic Search Algorithm. Nucl. Eng. Des. 2017. **311**:199–212.
22. Tran V.T., Tran H.N., Nguyen H.T., Hoang

V.K., Ha P.N.V. Study on Transmutation of Minor Actinides as Burnable Poison in VVER-1000 Fuel Assembly. Sci. Technol. Nucl. Install. 2019. **2019**

23. Lau C.W., Nylén H., Insulander Björk K., Sandberg U. Feasibility Study of 1/3 Thorium-plutonium Mixed Oxide Core. Sci. Technol. Nucl. Install. 2014. **2014**

24. Allen K., Knight T. Destruction Rate Analysis of Transuranic Targets in Sodium-Cooled Fast Reactor (SFR) Assemblies using MCNPX and SCALE 6.0. Prog. Nucl. Energy. 2010. **52**(4):387–94.

25. Fukaya Y., Goto M., Ohashi H., Tachibana Y., Kunitomi K., Chiba S. Proposal of a Plutonium Burner System Based on HTGR with High Proliferation Resistance. J. Nucl. Sci. Technol. 2014. **51**(6):818–31.

26. Ashraf O., Tikhomirov G. V. Thermal-and Fast-spectrum Molten Salt Reactors for Minor Actinides Transmutation. Ann. Nucl. Energy. 2020. **148**:107751.

27. Zou C., Yu C., Wu J., Cai X., Chen J. Parametric Study on Minor Actinides Transmutation in a Graphite-moderated Thorium-based Molten Salt Reactors. Int. J. Energy Res. 2020.:1–11.

28. Serp J., Allibert M., Beneš O., Delpech S., Feynberg O., Ghetta V., et al. The Molten Salt Reactor (MSR) in Generation IV: Overview and Perspectives. Prog. Nucl. Energy. 2014. **77**:308–19.

29. LeBlanc D. Molten Salt Reactors: A new Beginning for an Old Idea. Nucl. Eng. Des. 2010. **240**(6):1644–56.

30. Ignatiev V., Feynberg O., Gnidoi I., Merzlyakov A., Surenkov A., Uglov V., et al. Molten Salt Actinide Recycler and Transforming System without and with Th-U Support: Fuel Cycle Flexibility and Key Material Properties. Ann. Nucl. Energy. 2014. **64**:408–20.

31. Zou C., Yu C., Wu J., Cai X., Chen J. Ameliorating the Positive Temperature Feedback Coefficient for an MSR Fueled with Transuranic Elements. Ann. Nucl. Energy. 2021. **160**:108325.

32. Robertson R.C. *Conceptual Design Study of a Single-Fluid Molten-Salt Breeder Reactor.* 1971.

33. Li G.C., Cong P., Yu C.G., Zou Y., Sun J.Y., Chen J.G., et al. Optimization of Th-U fuel Breeding Based on a Single-fluid Double-Zone Thorium Molten Salt Reactor. Prog. Nucl. Energy. 2018. **108**(March):144–51.

34. Rykhlevskii A., Bae J.W., Huff K.D. Modeling and Simulation of Online Reprocessing in the Thorium-fueled Molten Salt Breeder Reactor. Ann. Nucl. Energy. 2019. **128**:366–79.

35. Waris A., Aji I.K., Pramuditya S., Novitrian, Permana S., Su'Ud Z. Comparative Studies on Plutonium and Minor Actinides Utilization in Small Molten Salt Reactors with Various Powers and Core Sizes. Energy Procedia. 2015. **71**:62–8.

36. Park J., Jeong Y., Lee H.C., Lee D. Whole Core Analysis of Molten Salt Breeder Reactor with Online Fuel Reprocessing. Int. J. Energy Researc. 2015. **39**:1673–80.

37. Silva C.A.M. da, Vieira A.L., Magalhães I.R., Pereira C. Neutronic Evaluation of MSBR System Using MCNP Code. Brazilian J. Radiat. Sci. 2021. **9**(2B):1–14.

38. Carter J.P., Borrelli R.A. Integral Molten Salt Reactor Neutron Physics Study using Monte Carlo N-Particle Code. Nucl. Eng. Des. 2020. **365**(February):110718.

39. Jaradat S.Q., Alajo A.B. Studies on the Liquid Fluoride Thorium Reactor: Comparative Neutronics Analysis of MCNP6 Code with SRAC95 Reactor Analysis Code Based on FUJI-U3-(0). Nucl. Eng. Des. 2017. **314**:251–5.

40. Khakim A., Rhoma F., Waluyo A., Suharyana S. The Neutronic Characteristics of Thermal Molten Salt Reactor. AIP Conf. Proc. 2021. **2374**(July):0–11.

41. Khakim A., Firmanda F.R., Pramono Y., Suharyana Assessment of TMSR-500 Shutdown Capability. Atom Indones. 2022. **48**(1):1–7.

42. Dwijayanto R.A.P., Oktavian M.R., Putra M.Y.A., Harto A.W. Model Comparison of Passive Compact-Molten Salt Reactor Neutronic Design Using MCNP6 and Serpent-2. Atom Indones. 2021. **47**(3):191–7.

43. Zou C.Y., Cai X.Z., Jiang D.Z., Yu C.G., Li X.X., Ma Y.W., et al. Optimization of Temperature Coefficient and Breeding Ratio for a Graphite-moderated Molten Salt Reactor. Nucl. Eng. Des. 2015. **281**:114–20.